DETERMINATION OF RED BLOOD CELL MEMBRANE VISCOSITY FROM RHEOSCOPIC OBSERVATIONS OF TANK-TREADING MOTION

R. TRAN-SON-TAY, S. P. SUTERA, AND P. R. RAO
Department of Mechanical Engineering, Washington University, St. Louis, Missouri 63130

ABSTRACT Measurements of the dimensions and membrane rotational frequency of individual erythrocytes steadily tank-treading in a rheoscope are used to deduce the surface shear viscosity of the membrane. The method is based on an integral energy principle which says that the power supplied to the tank-treading cell by the suspending fluid is equal to the rate at which energy is dissipated by viscous action in the membrane and cytoplasm. The integrals involved are formulated with the aid of an idealized mathematical model of the tank-treading red blood cell (RBC) (Keller and Skalak, 1982, *J. Fluid Mech.*, 120:24–27) and evaluated numerically. The outcome is a surface-averaged value of membrane viscosity which is representative of a finite interval of membrane shear rate. The numerical values computed show a clear shear-thinning characteristic as well as a significant augmentation of viscosity with cell age and tend toward agreement with those determined for the rapid phase of shape recovery in micropipettes (Chien, S., K.-L. P. Sung, R. Skalak, S. Usami, and A. Tozeren, 1978, *Biophys. J.*, 24:463–487). The computations also indicate that the rate of energy dissipation in the membrane is always substantially greater than that in the cytoplasm.

INTRODUCTION

The membrane of the human red blood cell (RBC) is recognized to possess remarkable mechanical properties. Together with the cytoplasmic fluid, which it contains, the membrane controls the overall deformability of the cell and, thus, its ability to traverse the microcirculation. Under normal flow conditions the RBC membrane deforms at constant area and exhibits both elastic and viscous behavior. It has been modeled reasonably well as an incompressible Kelvin solid characterizable by two material properties: the shear modulus of elasticity, μ_m, and the shear viscosity, η_m (Evans and Hochmuth, 1976). These properties have been successfully measured by means of delicate micropipette techniques in which portions of a cell's membrane are statically deformed under known loading and also allowed to recover after abrupt unloading. Evidence to date indicates that the moduli μ_m and η_m are variable, depending on shear strain and strain rate, respectively.

There is intense interest both in gross RBC deformability and membrane mechanical properties as potential indices of certain hematologic diseases. For this reason measurement techniques capable of rapidly processing large numbers of cells and thereby allowing statistical analysis are attractive. The ektacytometer (Bessis et al., 1980) is one device capable of qualitatively assessing shear-induced deformation averaged over thousands of cells instantaneously; however, its output is not amenable to quantitative deduction of membrane properties. Using the cone-plate rheoscope, it is possible to record simultaneously the motion and deformation of many tens or even hundreds of individual RBCs suspended in simple shear flow. The stationary state of motion called "tank-treading" has been well documented in the papers of Fischer and co-workers; see, for example, Fischer and Schmid-Schönbein (1977). As seen in the rheoscope, the tank-treading RBC assumes a flattened, quasi-ellipsoidal form while its membrane rotates steadily. In addition to the cell's elliptical periphery projected on the plane of shear, the translational speed of the membrane, made visible by marker beads, and thus its "tank-treading frequency," f, are directly measurable.

A primary objective of our work with the rheoscope is to deduce membrane properties from rheoscopic measurements on individual RBC. To accomplish this requires appropriate mathematical models which relate the desired properties to observable aspects of the tank-treading motion. The present paper describes an algorithm whereby a surface-averaged value of η_m can be calculated from rheoscopic data.

THEORY

The governing algorithm is based on a simplified but realistic model of the tank-treading RBC conceived by Keller and Skalak (1982). They represent the cell by an ellipsoidal energy-dissipating membrane encapsulating

Dr. Tran-Son-Tay's present address is the Department of Physiology and Biophysics, University of Southern California School of Medicine, 2025 Zonal Avenue, Los Angeles, CA.

an incompressible Newtonian liquid and immersed in a plane shear flow of a second incompressible Newtonian liquid. The membrane motion is prescribed in the form of a surface-velocity distribution which is kinematically similar to the motion observed in the rheoscope. Fig. 1 shows the model particle schematically and defines the coordinate systems and principal parameters of the flow. The *XYZ* axes are centered in the particle and oriented such that the undisturbed shear flow has components $\dot{\gamma}Y, 0, 0$ where $\dot{\gamma}$ is the shear rate. The *xyz* axes are the principal axes of the ellipsoid whose surface is defined by

$$x^2/a^2 + y^2/b^2 + z^2/c^2 = 1. \tag{1}$$

In the Keller-Skalak (K-S) model the prescribed membrane-velocity distribution is

$$\mathbf{U}^m = f[(a/b)y, -(b/a)x, 0], \tag{2}$$

where f is the tank-treading frequency, defined here as a positive constant (rad/s). The corresponding material trajectories are closed curves lying in planes z = constant, as depicted by the dashed lines in Fig. 1 *B*, and all membrane elements orbit synchronously with the same period $T = 2\pi/f$. Membrane markers attached to tank-treading cells are in fact observed to follow trajectories whose projections on the plane of observation (*X,Z*) are virtually straight lines (Fischer and Schmid-Schönbein, 1977). It should be pointed out that this simplified velocity field does not satisfy the condition of local area conservation. Nevertheless, in the interest of demonstrating the feasibility of this approach to the property η_m in the simplest possible manner we chose to work consistently within the framework of the K-S model. Later analytical work by Secomb and Skalak (1982) has shown that satisfaction of area conservation in an ellipsoidal membrane leads to velocity fields which are substantially more complex algebraically than Eq. 2, and it is not obvious that analytic solutions to the internal and external flow fields would even be feasible in such cases. This point is treated in greater detail under Discussion where we also describe an attempt to estimate the quantitative impact of using the simplified field of the K-S model.

The basis of an explicit equation for η_m is provided by an energy balance also enunciated by Keller and Skalak (1982): The power supplied to the tank-treading cell by the suspending fluid is equal to the rate at which energy is dissipated within the cell. The dissipation occurs within both the membrane and the cytoplasmic fluid and so we write

$$W_p = D_c + D_m, \tag{3}$$

where W_p is the power input, and D_c and D_m are the dissipation rates in the cytoplasm and membrane, respectively. All three of these terms depend on the details of the membrane velocity field. The first two terms were calculated by Keller and Skalak (1982) for the particular velocity field, Eq. 2. In slightly modified notation they are expressed here as

$$W_p = V\eta_0(f_2 f^2 + f_3 \dot{\gamma} f \cos 2\theta), \tag{4}$$

$$D_c = V\eta_i f_1 f^2, \tag{5}$$

where V is the ellipsoid volume, η_0 and η_i are external and internal fluid viscosities, respectively, θ is the angle of inclination of the ellipsoid with respect to the *X*-axis (Fig. 1), and f_1, f_2, f_3 are geometrical factors defined by

$$f_1 = \left[\frac{b^2 - a^2}{ab}\right]^2, \tag{6}$$

$$f_2 = f_1\left[1 - \frac{2}{\gamma_0' abc(a^2 + b^2)}\right], \tag{7}$$

$$f_3 = -\frac{2(a^2 - b^2)}{a^2 b^2 c \gamma_0'(a^2 + b^2)}, \tag{8}$$

and

$$\gamma_0' = \int_0^\infty \frac{d\lambda}{(a^2 + \lambda)^{3/2}(b^2 + \lambda)^{3/2}(c^2 + \lambda)^{1/2}}. \tag{9}$$

Let us recall that in the typical rheoscope experiment $\dot{\gamma}$ is an imposed, i.e., independent variable, and the frequency, f, is directly observable (by means of membrane markers). The lengths $a \cdot \cos\theta$ and c are also directly observed but are measured, in our system, only within an unknown scale factor. (This point is discussed in more detail in Experimental Method, below.) The external viscosity η_o is controlled, while η_i is well defined, at least for normal human cells, by the mean corpuscular hemoglobin concentration (MCHC) and the temperature. Thus, to calculate W_p and D_c, three more independent conditions involving the parameters a, b, θ, and the length-scale factor are necessary. One is provided by an equation for the equilibrium angle of inclination (Sutera and Tran-Son-Tay, 1983)

$$\cos 2\theta = [a^2 + b^2 - 4ab(f/\dot{\gamma})]/(a^2 - b^2). \tag{10}$$

A second condition obtains by specifying the surface area of the ellipsoid. In the case of a tri-axial ($a \neq b \neq c$) ellipsoid the area can be expressed directly in terms of elliptic integrals (Lévy, 1898) or, alternatively, as an infinite series (Keller, 1979). For our purposes the latter proved to be the more computationally convenient. Thirdly, we imposed the volume $V = (4\pi/3)abc$. With the addition of these two geometric conditions we can solve five algebraic equations simultaneously for a, b, c, θ, and the length-scale factor. Inserting these quantities into Eqs. 4 and 5 we can calculate W_p and D_c and, hence, the membrane-dissipation rate $D_m = W_p - D_c$. Now, D_m may be expressed as an integral over the membrane surface Σ of the rate of viscous dissipation per unit area

$$D_m = \iint_\Sigma E_v \, d\sigma, \tag{11}$$

where

$$E_v \equiv \eta_m' \Theta^2 + 2\eta_m \tilde{e}_{ij}^{(s)} \tilde{e}_{ij}^{(s)}, \tag{12}$$

η_m' and η_m are the coefficients of dilatational and shear viscosity, respectively, Θ is the rate of surface dilatation, and the $\tilde{e}_{ij}^{(s)}$ are the deviatoric components of the surface rate of strain tensor. [The superscript (s) signifies that the derivatives are taken in the curved surface Σ.] Secomb and Skalak (1982) have calculated the components of the surface strain rate in terms of the cartesian components of the membrane velocity, U_i^m, and the local unit normal vector, n_i:

$$e_{ij}^{(s)} = \frac{1}{2} P_{ik} P_{j\ell}\left(\frac{\partial U_k^m}{\partial x_\ell} + \frac{\partial U_\ell^m}{\partial x_k}\right), \tag{13}$$

$$P_{ij} = \delta_{ij} - n_i n_j. \tag{14}$$

The $e_{ij}^{(s)}$ expressed in Eq. 13 are the cartesian components of the complete surface tensor, including the rate of dilatation

$$\Theta = P_{ij}\frac{\partial U_i^m}{\partial x_j} = \frac{\partial U_i^m}{\partial x_i} - n_i n_j \frac{\partial U_i^m}{\partial x_j}. \tag{15}$$

The deviatoric components are defined by

$$\tilde{e}_{ij}^{(s)} = e_{ij}^{(s)} - \frac{1}{2}\Theta P_{ij}. \tag{16}$$

As previously mentioned, it is generally accepted that RBC membrane flow is essentially area-conserving, meaning that $\Theta \approx 0$. Hence, we will drop the dilatational term in Eq. 12. It may be argued that this step is inconsistent because the K-S velocity field does not satisfy the condition $\Theta = 0$ everywhere in Σ. It is indeed possible to calculate Θ for the K-S field

and retain its contribution to E_v, but, as a consequence, η'_m a second and presumably unknown material coefficient, would also be retained and would interfere with our objective of an explicit expression for η_m. In fact, the magnitude of η'_m is a key factor in the proposed truncation of E_v, for the ratio of the dilatational to the distortional term in E_v must be of order η'_m/η_m. It has been estimated (Evans and Hochmuth, 1978) that this ratio is very small, of order 10^{-3} - 10^{-4}.

By neglecting the dilatational contribution to D_m the energy balance reduces to an integral equation in one unknown, η_m. Rigorous solution of this equation would require knowledge of the functional dependence of η_m on shear rate. Although some experimental data bearing on this dependence have been reported (Chien et al., 1978), an adequate analytical characterization is not yet in hand. This being the case we take the expedient of dealing in terms of an integral average value of η_m, defined by

$$D_m = 2\iint_\Sigma \eta_m \tilde{e}_{ij}^{(s)} \tilde{e}_{ij}^{(s)}\, d\sigma \equiv 2\bar{\eta}_m \iint_\Sigma \tilde{e}_{ij}^{(s)} \tilde{e}_{ij}^{(s)}\, d\sigma. \quad (17)$$

As defined, $\bar{\eta}_m$ is a mean value corresponding to an interval of shear rate ranging from zero to an upper bound which is proportional to the applied shear rate. The maximum shear rates in the tank-treading membrane occur near the poles, P and P' in Fig. 1 (Fischer, 1980). With this last step, the energy balance can be rewritten as an explicit equation for $\bar{\eta}_m$:

$$\bar{\eta}_m = \frac{V[f^2(\eta_0 f_2 - \eta_i f_1) + f(\eta_0 \dot{\gamma} f_2 \cos 2\theta)]}{2\iint_\Sigma \tilde{e}_{ij}^{(s)} \tilde{e}_{ij}^{(s)}\, d\sigma}. \quad (18)$$

We evaluated the right member of this equation numerically in terms of the observed tank-treading frequency f, the applied shear rate $\dot{\gamma}$, the known viscosities η_o and η_i, and measurable geometrical parameters of the deformed cell.

EXPERIMENTAL METHOD

Rheoscope and Associated Optics

Direct microscopic observations and video recording of red cells tank treading at various shear stresses were accomplished by means of a counter-rotating cone-plate rheoscope (Schmid-Schönbein et al., 1973) (fabricated by K. Effenberger, Munich, Federal Republic of Germany). The transparent cone-plate shear chamber had a nominal angle of 1.5 degrees and was mounted on the stage of an inverted interference contrast microscope (Diavert, E. Leitz KG, 6330 Wetzlar, Federal Republic of Germany) with 100X objective. The microscope objective was focused at the midplane of the gap at a radial distance of ~1.5 mm from the center of rotation. The optical axis through the rheoscope corresponds to the y-axis of Fig. 1; hence the view observed is that of Fig. 1 *B*. A video camera (Dage-MTI, Inc., Wabash, MI, model 66, with plumbicon tube) framing at the range of 30 per second and synchronized to strobe illumination (Strobex 236B, Chadwick-Helmuth Co., Inc., El Monte, CA) transmitted images of the quasi-stationary cells to a videotape recorder (Sony Corp. of America, Long Island City, NY, Betamax SL 5800) for subsequent analysis. The applied shear rate is controlled through the rotational speed of the rheoscope and is calculated on the basis of an average gap between cone and plate. Owing to nonuniformities in the actual gap as well as experimental uncertainty in the rotational speed and the radial position of the field of observation, there is an estimated uncertainty associated with the applied shear rate of ±4% (Sutera et al., 1983).

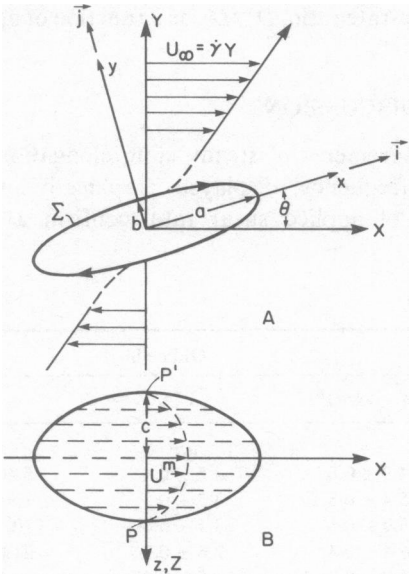

FIGURE 1 Diagram of the tank-treading ellipsoidal particle showing the notation used.

Preparation of RBC

All blood samples were taken from the same hematologically normal male donor. Blood was collected via venipuncture into 10-ml vacutainers containing 1 ml of 3.8% sodium citrate and centrifuged at 2,500 *g* for 10 min, thus concentrating the red cells to an hematocrit of 80% in the donor's plasma. Density separation was effected by short duration, high speed centrifugation according to the method of Laczko et al. (1979). Following centrifugation, the top and bottom 10% fractions were separated for study in the rheoscope. Because density correlates with age in normal RBC, these fractions correspond to the youngest and oldest 10% fractions, respectively. The cells were then washed twice in isotonic phosphate-buffered saline (PBS, 0.005 M KH_2PO_4 + Na_2PHO_4, pH = 7.40, 290 ± 5 mosmol/kg) plus 10 mM dextrose and 4 mM sodium citrate. After the second wash, the cells were resuspended in the same buffer minus sodium citrate plus 20% donor plasma at a 20% hematocrit. Finally, these fractions were diluted 10:1 by addition of suspending medium to an hematocrit of 2% for shearing in the rheoscope. All samples were tested within 8 h of venipuncture.

Suspending Medium

To achieve tank-treading at shear rates within the rheoscope's operating speed range, it was necessary to increase the viscosity of the PBS suspending medium by the addition of dextran polymer (molecular weight of 2×10^6, Sigma Chemical Co., St. Louis, MO). The dextran was dialyzed and freeze-dried to eliminate stomatocytic agents and dissolved in PBS buffer (minus citrate + 10 mM dextrose) in sufficient quantity to give a final suspension viscosity with 2% RBC of 35 ± 1 cP at room temperature, 22–24°C. The same medium was used throughout the experiments. The salt concentration in the medium was adjusted to give an osmolality of 290 ± 5 mosmol/kg, as determined by freezing-point depression.

0.035 Pa*s

Membrane Markers

To permit recording of membrane motion, polystyrene beads (1.0 μm, Dow Chemical Co., Indianapolis, IN) were added to the cell suspensions. These beads adhere well to the red cell membrane in the absence of plasma proteins. While the distribution of beads among cells was uncontrolled, an adequate number of cells with no more than two beads attached was usually obtained. Occasional cells with more than two beads were seen, but these were ignored in the determination of TTF. Fig. 2 is a photomicrograph of seven cells tank-treading in the rheoscope, two of which have single beads attached to their membrane.

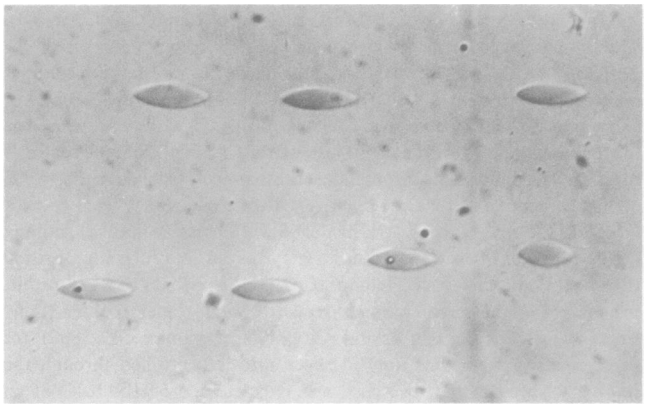

FIGURE 2 Photomicrograph of human red cells tank treading in the rheoscope. Cells suspended in PBS-dextran, applied shear rate = 200 s^{-1}. Polystyrene beads are attached to membrane of two cells.

Calculation of Tank-Treading Frequency (TTF)

The videotape was replayed frame-by-frame on a TV monitor (Audiotronics Corp., North Hollywood, CA, model 17M922) on whose screen was simultaneously displayed a digital reading of the time to the nearest millisecond. Observations were restricted to cells with a single attached bead. The time interval corresponding to a minimum of two complete revolutions of the marker bead was recorded, whence the period of one revolution, T, was computed. The reciprocal of T is the TTF in revolutions or cycles per second. The circular TTF in radians per second was finally calculated from the formula $f = 2\pi/T$. At each shear rate imposed, the TTF's of 30 different cells were so determined.

Length Measurements

Major and minor axes of the quasi-elliptical profiles of tank-treading cells were measured directly on the screen of the TV monitor by means of a video caliper (Vista Electronics, La Mesa, CA 92041 model 305 r). Owing to drift problems in this instrument it proved impracticable to calibrate caliper-indicated lengths directly against an absolute standard such as a grid. Instead, the diameter of a relaxed red cell located near the center of the viewing field was used as a calibration standard. This diameter was recorded initially as 8.0 μm. Subsequently, in the course of computations, the length calibration factor was adjusted upward or downward in order that the computed red cell volume matched a prescribed average value.

RESULTS

Red cell suspensions were sheared at five discrete shear rates, 28.6, 42.9, 57.1, 114.3, and 171.4 s^{-1}, corresponding to nominal shear stresses of 10, 15, 20, 40, and 60 dyn/cm^2. At each shear rate the tank-treading frequency, f, and the two lengths, $a \cdot \cos\theta$ and c, were measured for 30 different cells. The data obtained are summarized in Table I. The length data shown are uncorrected, i.e., based on a reference RBC diameter of 8.0 μm, as discussed above. The trends of f and the projected length-to-width ratio, $L_p/W \equiv a \cdot \cos\theta/c$, of the stretched RBC profile with increasing shear rate are displayed graphically in Fig. 3.

The average values presented in Table I were first used as inputs for digital computations of the corrected ellipsoid dimensions, a, b, and c, and the inclination angle, θ. In this process the membrane area and cell volume were assigned the following values based on the measurements of Nash and Wyard (1980): young cells, $S = 141\ \mu m^2$, $V = 111\ \mu m^3$; old cells, $S = 130\ \mu m^2$, $V = 99\ \mu m^3$. The results of these computations are collected in Table II. All computed lengths have been rounded to the nearest 0.1 μm.

The corrected geometrical quantities of Table II served as inputs for the final stage of computations which yielded the power input per cell, W_p, the cytoplasmic dissipation rate, D_c, the membrane-dissipation rate, D_m, and the surface-averaged membrane shear viscosity, $\bar{\eta}_m$. In these computations the cytoplasmic viscosity was initially assigned the value of 10 cP, considered to be a representative average value for red cells suspended in isotonic medium at room temperature (22°–24°C). In a subsequent computation we raised the cytoplasmic viscosity for the old cell fraction to 18 cP to model more realistically the effect of increasing mean corpuscular hemoglobin concentration with cell age. The results are given in Table III. Complete details of the computer programs used may be found in Tran-Son-Tay's dissertation (1983). The variation of $\bar{\eta}_m$ with applied shear rate is plotted in Fig. 4 for both young and old cell fractions. A final graph, Fig. 5, shows the dissipation-rate ratio, D_m/D_c, as a function of applied shear rate.

DISCUSSION

The measurements of steady state elongation and tank-treading frequency, displayed graphically in Fig. 3 as functions of applied shear rate, confirm a well-known

TABLE I
EXPERIMENTAL DATA*

	Young cells			Old cells		
$\dot{\gamma}$	$(a \cdot \cos\theta)$*	c*	f	$(a \cdot \cos\theta)$*	c*	f
s^{-1}	μm	μm	rad/s	μm	μm	rad/s
28.6	5.5 ± 0.5	3.2 ± 0.2	6.22 ± 0.31	4.9 ± 0.6	3.5 ± 0.4	5.40 ± 0.31
42.9	5.9 ± 0.7	3.0 ± 0.5	9.42 ± 0.57	5.4 ± 0.8	3.3 ± 0.3	7.98 ± 0.57
57.1	6.5 ± 0.8	2.5 ± 0.3	12.7 ± 0.57	5.9 ± 0.5	3.1 ± 0.4	10.5 ± 0.82
114.3	7.3 ± 0.4	2.3 ± 0.5	24.6 ± 1.07	6.4 ± 0.4	2.6 ± 0.3	21.0 ± 1.32
171.4	7.6 ± 0.4	2.1 ± 0.3	37.4 ± 1.45	6.9 ± 0.4	2.5 ± 0.2	30.8 ± 1.82

Means ± SD, $N = 30$.
*Uncorrected lengths, based on reference RBC diameter of 8.0 μm.

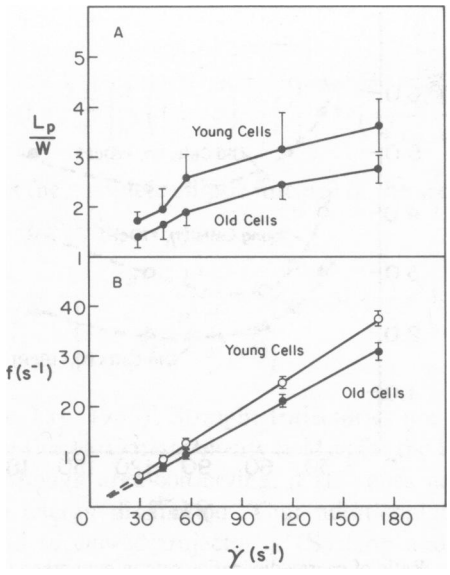

FIGURE 3 (*A*) Projected length-to-width ratio ($L_p = a\cos\theta$, $W = c$) and (*B*) tank-treading frequency (rad/s) vs. applied shear rate. Datum points are mean values for 30 cells; vertical bars are standard deviations.

age-related decline in gross cellular deformability. The reduced elongation of the older cells is indicative, at least partially, of a stiffer membrane, i.e., a higher shear modulus of elasticity. In fact, Linderkamp and Meiselman (1982), using the micropipette technique, found a 16% increase in the mean modulus of normal RBC with age. In contrast, the data plotted in Fig. 1 *A* show the average length-to-width ratio of the old cells running from 20 to nearly 40% below that of the young cells. This disproportionality is to be expected since the steady state deformation of the tank-treading RBC is a resultant of both elastic and viscous processes. In other words, the shear stresses exerted on the membrane by the external medium are opposed not only by elastic membrane stress but also by viscous stresses in both membrane and cytoplasm. The membrane shear viscosity is also reported to be elevated in old cells (Linderkamp and Meiselman, 1982), and this trend would further oppose elongation under steady shearing.

TABLE II
COMPUTED RESULTS: GEOMETRICAL PARAMETERS*

	Young cells $S = 141\ \mu m^2$, $V = 111\ \mu m^3$				Old cells $S = 130\ \mu m^2$, $V = 99\ \mu m^3$			
$\dot{\gamma}$	a	b	c	θ	a	b	c	θ
28.6	5.6	1.5	3.2	12.8	4.9	1.4	3.5	10.6
42.9	6.0	1.5	3.0	13.0	5.3	1.4	3.2	10.9
57.1	6.7	1.6	2.5	13.2	5.6	1.4	2.9	10.5
114.3	7.1	1.7	2.2	12.5	6.3	1.5	2.5	10.8
171.4	7.3	1.9	2.0	12.7	6.5	1.6	2.3	10.3

*a, b, c in microns, θ in degrees.

As shown in Fig. 3 *B*, the measured TTF is essentially proportional to applied shear rate over the range covered, and even though a finite level of shear stress must be applied to induce steady-state tank treading, the plotted mean values are seen to fall very nearly on a line through the origin. The difference in the slopes of the two lines, 0.22 and 0.18 for the young and old cells, respectively, is highly significant statistically and agrees precisely with the result of our recent investigation of variance in TTF in normal human RBC (Sutera et al., 1983). In accordance with our premise of a balance between work input and viscous dissipation in the steadily tank-treading RBC, we attribute the decrease in TTF with age to an increase in membrane and/or cytoplasmic viscosity.

The cytoplasmic viscosity is determined by the mean corpuscular hemoglobin concentration (MCHC) which increases in inverse proportion to the decreasing volume of the aging erythrocytes. As a consequence of the strongly nonlinear relationship between viscosity and concentration of hemoglobin solutions (Ross and Minton, 1977) the viscosity rises rapidly once the MCHC exceeds 30 g/dl. According to the Ross-Minton model the viscosity of 10 cP at room temperature corresponds approximately to a concentration of 33.5 g/dl. (This assumes that the viscosity of hemoglobin solutions has about the same temperature dependence as that of water.) Corresponding then to the 12% decrease of mean cell volume postulated in our computations (111 to 99 μm^3) the MCHC would increase to 37.5 g/dl in the old cell fraction. For this concentration the Ross-Minton model gives $\eta_i = 13.2$ cP at 37°C or roughly 18 cP at room temperature. This value was the basis for the second series of computations carried out to test the influence of this parameter on the membrane viscosity.

The computations of surface-averaged membrane viscosity, $\bar{\eta}_m$, clearly show a decreasing trend with increasing applied shear rate (Fig. 4), i.e., a shear-thinning behavior. The effect of increasing the cytoplasmic viscosity from 10 to 18 cP was predictable: lower rates of dissipation in the membrane and, hence, lower membrane viscosities. Even so, there remains a substantial increment in the membrane viscosity, on the order of 40% in the asymptotic range. This compares with a 76% increment found by Linderkamp and Meiselman (1982). On the other hand, their viscosities, obtained by the micropipette-recovery time technique, exceed the values of $\bar{\eta}_m$ derived from the present semi-empirical approach by about one order of magnitude. However, Chien et al. (1978) have reported values down to 0.6×10^{-4} dyn·s/cm for the initial rapid phase of recovery from micropipette aspiration, in excellent agreement with our lowest computed values of $\bar{\eta}_m$. They further calculated that their lowest values of viscosity corresponded to rates of shear strain in the range 100 to 300 s^{-1}, approximately. By means of a rough order-of-magnitude estimate, we can show that the rate of shear strain in the membrane of the tank-treading RBC is comparable. Consider the case of an

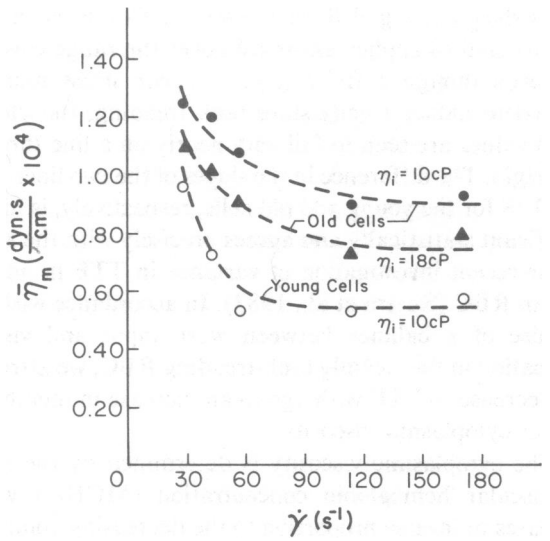

FIGURE 4 Average membrane shear viscosity vs. applied shear rate. Plotted points are computed values based on data averaged over 30 cells.

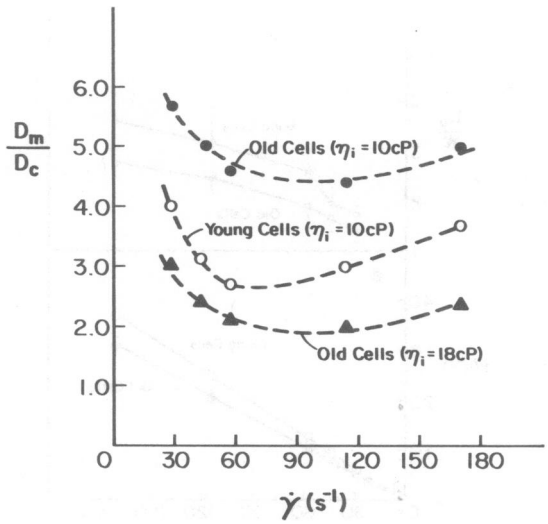

FIGURE 5 Ratio of energy-dissipation rate in membrane (D_m) to energy-dissipation rate in cytoplasm (D_c). Plotted points are computed values based on data averaged over 30 cells.

average young cell tank-treading at the highest applied shear rate, 171 s^{-1}. Its TTF is 37 rad/s or ~6 rev/s (Fig. 3 *B*), so the half-period of a material point is 1/12 s. The length of the major axis of the cell ($2a$) is ~15 μm (Table II). Thus the average velocity of membrane elements moving along the central streamline (in the xy-plane of Fig. 1) is of order 15/(1/12) = 180 μm/s. The distance from this streamline to the poles is c = 2 μm (Table II). The quotient of average velocity over this distance, 90 s^{-1} gives the order of magnitude of membrane shear rate. Corresponding to this condition the computed $\bar{\eta}_m$, 0.57 × 10^{-4} dyn·s/cm (Table III), is in virtual agreement with the findings of Chien et al. (1978).

The energy-dissipation rates, D_m and D_c (Table III), were both found to increase strongly with applied shear rate or, equivalently, TTF, as found by Fischer (1980). The plots of the ratio, D_m/D_c (Fig. 5), reveal that the membrane is the dominant energy sink over the entire range of shear rate covered. As shown by the two sets of values computed for the old cells (η_i = 10, 18 cP), the ratio is strongly sensitive to the cytoplasmic viscosity. We do not have an explanation for the apparent minimum in the variation of D_m/D_c with TTF. We note that Fischer's calculated ratios (1.0 to 2.8) are in order-of-magnitude agreement with ours. However, the two sets of numbers should not be too closely compared, as Fischer's computations were based on different cell surface and volume.

Finally, let us return to the subject of the membrane velocity field. As pointed out under Theory, the simplified field of the K-S model does not obey the constraint of local area conservation. We wished to estimate the effect of this "error" in the mathematical model on the results obtained. Secomb and Skalak (1982) have analyzed the kinematics of area-conserving surface flows and shown that the velocity field

$$\mathbf{U}^m = \frac{f F'(z)}{\sqrt{x^2/a^4 + y^2/b^4 + z^2/c^4}} \left(\frac{y}{b^2}, -\frac{x}{a^2}, 0 \right) \qquad (19)$$

satisfies local area conservation on the ellipsoidal surface, Eq. 1. The function $F'(z)$ is determined by the condition of synchrony, i.e., that all material points execute cyclic motions with one common frequency, f. For the ellipsoidal

TABLE III
COMPUTED RESULTS: ENERGETIC PARAMETERS AND AVERAGE MEMBRANE VISCOSITY

	Young cells (η_i = 10 cP)				Old cells (η_i = 10 cP)				Old cells (η_i = 18 cP)			
$\dot{\gamma}$	W_p	D_c	D_m	$\bar{\eta}_m$	W_p	D_c	D_m	$\bar{\eta}_m$	W_p	D_c	D_m	$\bar{\eta}_m$
s^{-1}	$erg \cdot s^{-1} \times 10^6$			$(dyn \cdot s/cm) \times 10^4$	$erg \cdot s^{-1} \times 10^6$			$(dyn \cdot s/cm) \times 10^4$	$erg \cdot s^{-1} \times 10^6$			$(dyn \cdot s/cm) \times 10^4$
28.6	0.025	0.005	0.020	0.96	0.021	0.003	0.017	1.25	0.021	0.005	0.015	1.09
42.9	0.058	0.014	0.043	0.72	0.048	0.008	0.040	1.20	0.048	0.014	0.034	1.01
57.1	0.103	0.028	0.074	0.53	0.084	0.015	0.069	1.08	0.084	0.027	0.058	0.90
114.3	0.417	0.104	0.313	0.53	0.364	0.067	0.294	0.90	0.364	0.123	0.241	0.72
171.4	0.985	0.209	0.776	0.57	0.834	0.138	0.696	0.93	0.834	0.249	0.585	0.79

surface

$$F'(z) = \frac{2ab}{\pi}\left[\frac{1}{b^2}\left(1 - \frac{z^2}{c^2}\right) + \frac{z^2}{c^4}\right]^{1/2} E\left(\sqrt{\frac{c_1}{c_2}}, \frac{\pi}{2}\right), \quad (20)$$

where E is the complete elliptic integral of the second kind with the parameter

$$\frac{c_1}{c_2} = \frac{a^2 - b^2}{a^2\left\{1 + \dfrac{b^2 z^2}{c^4(1 - z^2/c^2)}\right\}}, \qquad 0 < \frac{c_1}{c_2} < 1, \quad (21)$$

(Tran-Son-Tay, 1983). Straight trajectories are a salient feature for this particular velocity field as for the K-S field, Eq. 2. Although area-conserving, it still does not satisfy minimum energy dissipation. That additional condition would lead to curved trajectories (Secomb and Skalak, 1982). Owing to its algebraic complexity, particularly its nonlinearity in the coordinates x, y, z, the velocity field represented by Eq. 19 cannot be accommodated as a boundary condition either in the K-S model or in our earlier calculation of the external velocity field (Sutera and Tran-Son-Tay, 1983). To solve the full problem with an area-conserving membrane velocity a numerical approach will undoubtedly be required. Short of such a major undertaking, some insight may be gained by examining the surface integral in the right member of Eq. 17 which, by definition, is proportional to the membrane dissipation rate. The values of D_m and $\bar{\eta}_m$ contained in Table III stem from the K-S model. We recomputed the surface integral using the Secomb-Skalak (S-S) area-conserving field, Eq. 19, inserting the same values of the parameters f, a, b, and c corresponding to the young cells. The results are seen in Table IV along with the same integral computed with the K-S velocity field. We find that the area-conserving velocity field results in smaller values, between 60 and 70% of those obtaining with the K-S field. Hence, for the same global rate of dissipation in the membrane, D_m, the area-conserving velocity field would lead to predictions of $\bar{\eta}_m$ roughly 40–70% greater than those computed for the K-S model (Table III, young cells). Of course, there is no basis for arguing that the difference between the rates W_p and D_c, i.e., D_m, would be the same were the full problem solved for the S-S velocity field. Nevertheless, taking into account the integral nature of the quantities W_p, D_c, and D_m, we would certainly expect them to retain the same order of magnitude at corresponding shear rates, even though the details of the membrane velocity distribution are changed. Accordingly, we feel that the surface-averaged membrane viscosity computed on the basis of the K-S model is of the correct magnitude but probably underestimates the true range by something less than a factor of 2.

TABLE IV
COMPARISON, COMPUTED VALUES* OF SURFACE INTEGRAL, EQ. 17, BASED ON K-S AND S-S MEMBRANE VELOCITY FIELDS

$\dot{\gamma}$ s^{-1}	$\iint_\Sigma \tilde{e}_{ij}^{(s)}\,\tilde{e}_{ij}^{(s)}\,d\sigma$	$[(cm^2/s^2) \times 10^2]$
	K-S	S-S
28.6	0.021	0.014
42.9	0.060	0.038
57.1	0.142	0.086
114.3	0.591	0.373
171.4	1.361	0.933

*Based on values of f, a, b, c for young cells, Table II.

CONCLUSION

In summary, we have demonstrated the feasibility of deducing a key mechanical property of the RBC membrane from rheoscopic observations of individual erythrocytes in steady state tank treading. This accomplishment enhances the utility of the rheoscope as a quantitative tool. The apparent agreement between the numerical values of membrane shear viscosity obtained through this semi-empirical method based on an energy principle with those based on micropipette shape-recovery measurements supports the validity of both approaches. Since the tank-treading cells are free of contact with any foreign surface, this agreement further tends to dispel concern about a surface-contact artifact in the micropipette measurement.

The helpful advice of Professors R. A. Gardner and G. I. Zahalak is gratefully acknowledged. We are indebted to Mr. C. W. Boylan for his expert technical assistance in the execution of the experiments.

This work was supported by research grant HL-12839 from the National Heart, Lung, and Blood Institute.

Received for publication 17 August 1983 and in final form 20 December 1983.

REFERENCES

Bessis, M., N. Mohandas, and C. Feo. 1980. Automated ektacytometry: a new method of measuring red cell deformability and red cell indices. *Blood Cells.* 6:315–327.

Chien, S., K-L. P. Sung, R. Skalak, S. Usami, and A. Tozeren. 1978. Theoretical and experimental studies on viscoelastic properties of erythrocyte membrane. *Biophys. J.* 24:463–487.

Evans, E. A., and R. M. Hochmuth. 1976. Membrane viscoelasticity. *Biophys. J.* 16:1–11.

Evans, E. A., and R. M. Hochmuth. 1978. Mechanochemical properties of membranes. *Curr. Top. Membr. Transp.* 10:1–64.

Fischer, T. M. 1980. On the energy dissipation in a tank-treading red blood cell. *Biophys. J.* 32:863–868.

Fischer, T. M., and H. Schmid-Schönbein. 1977. Tank tread motion of red cell membranes in viscometric flow: behavior of intracellular and extracellular markers. *Blood Cells.* 3:351–365.

Hochmuth, R. M. 1980. Viscoelastic solid behavior of red cell membrane. *In* Erythrocyte Mechanics and Blood Flow. G. R. Cokelet, H. J. Meiselman, and D. E. Brooks, editors. Alan R. Liss, Inc., New York. 57–74.

Keller, S. R. 1979. On the surface area of the ellipsoid. *Math. Comp.* 33:310–314.

Keller, S. R., and R. Skalak. 1982. Motion of a tank-treading ellipsoidal particle in a shear flow. *J. Fluid. Mech.* 120:24–27.

Laczko, J., C. Feo, and W. Phillips. 1979. Discocyte-echinocyte reversibility in blood stored in CPD over a period of 56 days. *Transfusion.* 19:379–388.

Lévy, L. 1898. Précis élémentaire de la théorie des fonctions élliptiques. Gauthier-Villars, Paris. 148.

Linderkamp, O., and H. J. Meiselman. 1982. Geometric, osmotic and membrane mechanical properties of density-separated human red cells. *Blood.* 59:1121–1127.

Nash, G. B., and S. J. Wyard. 1980. Changes in surface area and volume measured by micropipette aspiration for erythrocytes ageing in vivo. *Biorheology.* 17:479–484.

Ross, P. D., and A. P. Minton. 1977. Hard quasispherical model for the viscosity of hemoglobin solutions. *Biochem. Biophys. Res. Commun.* 76:971–976.

Schmid-Schönbein, H., J. Gosen, L. Heinich, H. J. Klose, and E. Volger. 1973. A counter-rotating rheoscope chamber for the study of the microrheology of blood cell aggregation by microscopic observation and microphotometry. *Microvasc. Res.* 366–376.

Secomb, T. W., and R. Skalak. 1982. Surface flow of viscoelastic membranes in viscous fluids. *Q. J. Mech. Appl. Math.* XXXV. 2:233–247.

Sutera, S. P., and R. Tran-Son-Tay. 1983. Mathematical model of the velocity field external to a tank-treading red cell. *Biorheology.* 20:267–282.

Sutera, S. P., R. Tran-Son-Tay, C. W. Boylan, J. R. Williamson, and R. A. Gardner. 1983. A study of variance in measurements of tank-treading frequency in populations of normal human red cells. *Blood Cells.* 9:485–495.

Tran-Son-Tay, R. 1983. A study of the tank-treading motion of red blood cells in shear flow. D.Sc. dissertation. Department of Mechanical Engineering. Washington University, St. Louis, MO.